

GPO PRICE \$ _____

CFSTI PRICE(S) \$ _____

Hard copy (HC) 1.00

Microfiche (MF) 150

ff 653 July 65

RECENT RESEARCH RESULTS IN THE AERODYNAMICS OF SUPERSONIC VEHICLES


By A. Warner Robins, Head, Supersonic Mechanics Section,
Odell A. Morris and Roy V. Harris, Jr., Aerospace Engineers

Large Supersonic Tunnels Branch
NASA, Langley Research Center
Langley Station, Hampton, Va.

Presented at the AIAA/RAeS/JSASS Design and Technology Meeting

FACILITY FORM 802	N66 29374	_____
	(ACCESSION NUMBER)	(THRU)
	20	1
	(PAGES)	(CODE)
	TMX-56865	01
	(NASA CR OR TMX OR AD NUMBER)	(CATEGORY)

Los Angeles, California
November 15 - 18, 1965



RECENT RESEARCH RESULTS IN THE AERODYNAMICS OF SUPERSONIC VEHICLES

By A. Warner Robins, Head, Supersonic Mechanics Section,
Odell A. Morris and Roy V. Harris, Jr., Aerospace Engineers

Large Supersonic Tunnels Branch
NASA, Langley Research Center

ABSTRACT

29374

The continuing aerodynamic-research effort aimed at improving the design of supersonic-cruise vehicles has recently produced some significant results. Research by both government and industry has provided, in addition to a better understanding of the design problem itself, some new and very useful design tools and concepts. Some of the advantages of these methods in the treatment of wave drag and drag due to lift are briefly discussed. Also presented are some new considerations of aerodynamic interference and its effect on the aerodynamic efficiency of the trimmed vehicle. An illustrative example of the application of these design tools and concepts to the aerodynamic design of a supersonic-cruise vehicle (SCAT 15-F) is made. A parallel analytic and experimental buildup of the vehicle is presented including treatment of the symmetric (flat camber-plane), the warped, and the warped-and-reflexed versions of the configuration. The potential of the new techniques is demonstrated by the good agreement between experiment and theory and by the high level of vehicle performance.

INTRODUCTION

A basic aim of aerodynamic research is to provide the design aerodynamicist with rational, rapid, and reliable means for evaluating the aerodynamics of a given aerodynamic shape and to enable him to quickly assess the cost in aerodynamic efficiency of proposed changes in vehicle shape brought about by other considerations. A short reaction time for the aerodynamicist will permit him to participate more effectively at the vehicle concept stage and thus provide for a much more comprehensive design process. Intensive effort by both government and industry has therefore been devoted

L-4747

to the implementation of existing theory with new analytical and numerical methods such that the high-speed computer might provide calculative results heretofore restricted to certain relatively simple shapes. Some significant contributions to this end have recently been made. These with other new considerations of the aerodynamics of the supersonic vehicle will be discussed.

DISCUSSION

Zero-lift wave drag.- One of the most useful developments has been the application of the high-speed computer to the problem of rapidly determining the zero-lift wave drags of highly complex shapes. Earlier efforts had depended upon graphical or semigraphical schemes for generation of the geometry of the many equivalent bodies and utilized, with erratic results, a Fourier series representation of the slopes of areas of these bodies in the drag calculations. More recent schemes accomplish the geometric exercise with the computer using a mathematical model of the aircraft as shown in figure 1 and determine the drag of the equivalent bodies as represented by least-drag paths through the computed cross-section areas. The result is a significant advancement in both speed and accuracy. The right-hand portion of the figure shows the agreement between calculated and experimental values in the Mach number range from 1.4 to 3.2 for very complex, complete configurations designed for supersonic cruise, varying from fighter-type vehicles on the upper right to bomber and transport types on the left. Except for the three high points, all of which may have resulted from boundary-layer separation, the agreement is generally good. Such computer programs certainly represent a powerful aid to the design aerodynamicist.

Design of the supersonic wing.- Another important application of the high-speed computer to supersonic aerodynamics has removed two rather severe limitations to supersonic wing design. The most obvious restriction eliminated involved wing planform; where once only simple planforms could be readily handled, essentially arbitrary planforms may now be treated (see references 1 and 2). The other limitation was the "inverse" problem -- that is; given the wing planform and wing warp, find the load distribution. The ability to [REDACTED] wing warp, given the planform and the design lift

coefficient, had long since been possible for simple planforms. This last limitation had led to some confusion. Since the theory as applied to the common arrow wing, for example, called for extreme slopes of the root chord, as seen in figure 2, and since these slopes could never be faithfully represented experimentally for obvious reasons, no real check of the theory, as applied to warped wings, could be made. The difference between the theoretical and real wings lay within a small region of the planform near the plane of symmetry and was rather generally thought to be of little consequence. The drag polars on the left in the figure show typical lack of agreement between experiment for the real wing and theory for the theoretical wing. In contrast (but not shown here) experiment and theory generally showed good agreement for the flat wing. The theoretical flat-wing and lower-bound polars are shown here for reference. It should be noted that the lower bound curve represents the envelope of polars for a family of wings each having optimum warp for a different lift coefficient. With the removal of the "inverse" restriction, however, the new computer program has enabled, for the first time, the comparison of the theoretical and experimental values for the real wing as shown on the right. Thus it is seen that the previous disparities were not because the theory had failed to represent the real flow, but rather because we had been failing to represent the shapes prescribed by theory. Thus it is seen that not only may we compute the loading of a complex wing shape at on-design and off-design conditions, but that, for reasonable degrees of camber-plane warp, the linear theory on which the computer programs are based may be expected to yield reliable results.

Effects of wing warp. - There are two characteristics of the warped or twisted and cambered wings which are important to the design aerodynamicist. Generally the warped wing provides an increment in maximum lift-drag ratio due to improved lifting efficiency, $\frac{dC_D}{dC_L^2}$, and a positive pitching-moment at zero lift (C_{m_0}). This is particularly applicable in the case of the wing with subsonic leading edges. These characteristics are a function of design-lift coefficient (or degree of wing warp) as shown in figure 3. Note that, at extreme wing design-lift coefficients, the theory is unable to faithfully represent the real flow over the highly distorted wing surfaces. Note also that the $C_{L_{design}} = .08$ wing and the $C_{L_{design}} = .16$ wing are superior in both respects to the $C_{L_{design}} = 0$ or

flat wing. These data are from reference 3. Figure 4 shows what this means in terms of the maximum trimmed lift-drag ratio, the important airframe flight-efficiency parameter at any given Mach number and stability margin. Here, maximum trimmed lift-drag ratio is plotted as a function of stability margin for wing-body combinations which, except that one has a flat and the other a warped wing camber plane, are otherwise identical. The important thing to note here is not so much the difference between the maximum lift-drag ratio (between points A and B) as seen in the previous figure, but the difference, due to the pitching moment increment, in maximum trimmed lift-drag ratios at some reasonable level of positive stability (between points A and C). This will be noted again later.

Supersonic aerodynamic interference.- It is certain that the designer of the efficient supersonic-cruise vehicle cannot settle for the thin-element or zero-interference case; the configuration must fit together in such a way that the drag of the aggregate is substantially less than that of the isolated components. Put another way; the avoidance of adverse interference will not be good enough. Because it is not known to be adequately treated elsewhere, much of the remainder of this paper will deal with this subject. The absence of systematic data requires a qualitative treatment using simple, rather obvious examples. The next series of figures then will be concerned with interference between components consisting of a double-wedge-section wing semispan and several cones which might be considered equivalent-body representations of engine nacelles.

Figure 5 represents the no-interference case -- disturbances produced by any component are not felt by any other component. Representative variations of pitching-moment and drag coefficients with lift coefficient and of maximum trimmed lift-drag ratio with longitudinal stability are shown in the lower portion of the figure. In figure 6 the components are arranged so that the compressions from the cones fall upon the receding slopes of the wing and the expansions from the wing impinge upon the advancing portions of the cones. Here the components are helping one another along. This favorable drag interference is reflected in the drag polars at bottom left where the curves from the previous no-interference case are represented by the dashed lines and the present case with the solid lines. The compressions from the cones also impose

an interference lift along the aft portions of the wing so that a nose-down or negative pitching-moment increment is present as shown in the curves at lower left. Note that, in the limit and neglecting viscous forces, the arrangement of components shown in this figure might be represented by the wing with the attached wedge as shown in the sketch at right and that this is a trailing-edge-down condition. Thus maximum trimmed lift-drag ratio occurs in the unstable region and considerable control deflection might be required for trimmed flight at positive stability. In fact, depending on the type of longitudinal controls, it is very possible that this favorable-interference case might be less efficient at reasonable stability levels than the zero-interference arrangement as is shown on the lower right. Figure 7 represents a favorable-interference case in which wing reflex has been employed. The characteristics of the two previous cases are shown as broken lines and are compared with the solid lines of the present case in the lower part of the figure. First, however, the configuration sketch should be examined. Note that the airfoil is no longer symmetric -- that, as noted previously, the airfoil has been reflexed, providing a steeper lower-surface slope which facilitates drag cancellation, between the lower surface and the cones, and that the wing upper-surface slope is reduced, lowering its pressure drag. Again note the sketch of the approximately-equivalent configuration on the right. Note that, with the wing reflexed and the cones represented by the attached wedge, the result is a symmetric, slab-trailing-edge wing which has a still lower drag than the previous or trailing-edge-down arrangement and a pitching-moment curve such as that of the original, no-interference case. Of interest is the fact that a wing thus reflexed approaches the case of an unreflexed, transparent wing in which perturbations from an interference source on one side of the wing are able to pass freely through the wing, effecting pressures on both upper and lower surfaces. This, incidentally, is the way the wave-drag computer program sees it and is why the combination of a reflexed wing and its interference body may be adequately represented to the computer by the geometry of the unreflexed wing and the interference body. It is also interesting to note that wing reflex which is designed to accommodate an interference body in the presence of an "optimum" wing can cancel the lift interference due to that body, preserving the lift distribution originally designed into the unreflexed wing. In any event, referring to

the lower right in figure 7, the slightly lower drag and the cancellation of the adverse pitching-moment interference provide that the maximum trimmed lift-drag ratio of the arrangement with favorable interference and wing reflex can be substantially superior to the other two at reasonable levels of stability.

Figure 8 provides a review of the previous discussion of interference and relates it to the earlier consideration of wing warp. Progress in the use of interference can be traced from zero-interference, through favorable interference, to favorable interference with wing reflex. Recalling now that the warped wing can provide lower drag at lift and a positive increment in pitching moment as shown here, application of the favorable interference with wing reflex to the warped wing can provide, at reasonable stability margins, a very large gain in maximum trimmed lift-drag ratio. Thus it is seen that favorable interference can provide improvements in maximum lift-drag ratio while producing decrements in our airframe flight-efficiency parameter at normal stability levels, but that with proper application (including wing reflex) substantial overall benefits can be realized.

The actual application of wing reflex in order to accommodate nacelle interference might be as shown in figure 9. The regions of influence of the nacelles depend primarily on Mach number and lift coefficient and may be satisfactorily defined using nacelle geometry or nacelle equivalent-body geometry and a number of calculative methods including the method of characteristics, Whitham's modified linear theory, or the cone tables. The interference pressures may be calculated satisfactorily using either of these theories, or an empirical scheme accounting for the total interference lift might be used. Calculation of the slope changes necessary to relieve the wing of the interference pressures, where these pressures are provided in detail, will oftentimes result in steep local slopes which, even if the theory perfectly matches the real flows, will operate correctly at the one design Mach number and lift coefficient. A reflex shape falling somewhere between this theoretical one and one which results from a linear reflex designed to cancel the total, not the local, interference load will probably be satisfactory. A typical section through the reflexed region of the wing might be as shown at the bottom of the figure.

Effects of sidewash.- Another effect of the installation on the wing of bodies such as nacelles or stores or of struts, fences or fins, is shown in figure 10. The bodies are shown with "toe-in" out of consideration of the sidewash beneath the lifting wing at design condition. The high drag increment at the negative-lift condition comes from the rather extreme misalignment of the bodies, thus oriented, with the underwing sidewash. At some positive lift coefficient, they become essentially aligned with the flow and at slightly higher values, some thrust component of the body side-force might be generated. A very simple analysis, which neglects body volume effects and the interference of the pressure fields associated with the body-sidewash misalignment, would have the body be set at half the local sidewash angle. In any event, it should be remembered, particularly when examining the drag polar of a complex configuration, that, as lift coefficient is changed, dramatic changes in the drag increment due to nacelle, stores, fins, and the like, can occur. These effects should not be confused with those of the interference previously discussed.

Sample application.- Figure 11 shows an aircraft configuration which was designed, using the several previously discussed tools and concepts, with a view to focusing attention on these developments. The configuration, SCAT 15-F, nominally represents a long-range supersonic transport vehicle having a cruise Mach number near 2.7. In the generation of the configuration, certain fundamental points, in accordance with the foregoing discussions, seemed apparent. It appeared that the wing-fuselage-nacelles combination should be self-trimming and that the drag due to lift should be lower than the flat plate value (these points, of course, are interrelated). Further; the components of the configuration should go together so as to provide, as previously noted, for maximum beneficial interference; and, more fundamentally, those components should either lift or thrust or be, if not altogether eliminated, at least minimized. These considerations tended to lead to a configuration having a largely subsonic leading edge and some trailing edge notch -- the latter so as to reduce the low-grade lifting surface falling in the downwash of the remainder of the wing. Also, such requirements tend to lead to a warped wing so as to provide the least drag in trimmed flight at the design point. The interference considerations virtually dictated that the engine nacelles be located beneath

and rearward on the wing. The minimization of non lifting or non-thrusting surfaces eliminated the separate horizontal tail and provided that the vertical fins be placed outboard, as shown, in a region of high effectiveness. Thus the basic concept was set. It remained to analytically exercise the concept so as to establish the trade sensitivities necessary to optimizing the aerodynamic shape.

While the shaping of the configuration with the use of the aforementioned analytic tools and concepts was generally rather straightforward, one particular consideration in the process which has not been previously mentioned is worthy of note. This has to do with integration of the wing-fuselage combination and involves the elimination of fuselage forebody lift and the consequent viscous cross-flow on that forebody at design-lift conditions. Such cross-flow tends to greatly exceed the design values of local upwash at the wing-root leading-edge; a matter of great importance since the lifting efficiency of the wing is critically dependent, for the establishment and spanwise growth of the proper upwash along the wing leading edge, upon achieving correct upwash at the wing root. This being the case, the wing planform considered when calculating the optimum wing warp had to have a blunted apex (since we have said that the forebody which contains the basic arrow-shaped apex may carry no lift and, hence, should be neglected). The actual apex selected was parabolic with the required forebody droop initiating at its origin.

Once the configuration geometry was defined, three wind-tunnel models were constructed. One of these, of course, represented the complete configuration with a warped and reflexed wing, engine nacelles and vertical tails. The other two were designed to provide, with the first, a complete, step by step, experimental buildup as set forth in the foregoing discussions. They were, therefore, a wing-body configuration having a flat camber plane and a wing-body combination with wing warp identical to the complete configuration except that no wing reflex was employed. The results of the analytic and experimental tests are shown in figure 12. No pitching-moment data are shown here, the important comparison in this regard having been shown in figure 4 which contained data from the tests from which these data are taken and which demonstrated the significant benefits of wing warp. This figure traces, in terms of lift-drag polars, the evolution of the configuration through the flat wing-body combination, the warped wing-body combination, the warped wing-body

configuration with vertical tails, to the complete configuration with its reflexed, warped wing. The reference drag polar is that of the warped wing-body combination which represents essentially the best that can be done with the configuration without nacelles and vertical tails. In the comparison on the left the warped wing is seen to be superior, as expected, to the flat wing, although, as noted previously, the most significant benefit of the wing warp is seen in trimmed lift-drag ratio (figure 4). In the middle figure, the addition of the vertical tails is seen to produce very little, if any, drag penalty at lift as would be indicated by earlier discussion. In the right-hand figure, the addition of the vertical surfaces and the four engine nacelles with wing reflex is seen to produce a considerable drag decrement near zero lift which diminishes as lift increases. It is interesting to note that, in addition to the trimming advantages noted earlier, the drag of the complete configuration with all its components is less than that of the flat-wing-body combination alone at and above cruise lift. The agreement between theory and experiment for the complete configuration is not as good as that of the others due in part, no doubt, to the fact that the theory, although it accounts for the drag due to sidewash of the nacelles and tails themselves, does not account for the distortion of the lift distribution caused by the pressure fields associated with the lateral loads on these components. The overall agreement between experiment and theory, however, is very good, which, when coupled with the fact that very high lift-drag ratios were attained, attests to the usefulness and soundness of the analytic processes and concepts used.

SUMMARY

In summary, some very useful, well implemented analytic processes have been developed which promise to greatly improve the speed and reliability with which the supersonic aerodynamics of a configuration may be evaluated. Application of these processes in conjunction with proper treatment of component interference should lead to substantial improvements in the performance of supersonic-cruise vehicles.

REFERENCES

1. Middleton, Wilbur D., and Carlson, Harry W.: A Numerical Method for Calculating the Flat-Plate Pressure Distributions on Supersonic Wings of Arbitrary Planform. NASA TN D-2570, January 1965
2. Carlson, Harry W., and Middleton, Wilbur D.: A Numerical Method for the Design of Camber Surfaces of Supersonic Wings With Arbitrary Planforms. NASA TN D-2341, June 1964
3. Carlson, Harry W.: Aerodynamic Characteristics at Mach Number 2.05 of a Series of Highly Swept Arrow Wings Employing Various Degrees of Twist and Camber. NASA TM X-332, 1960

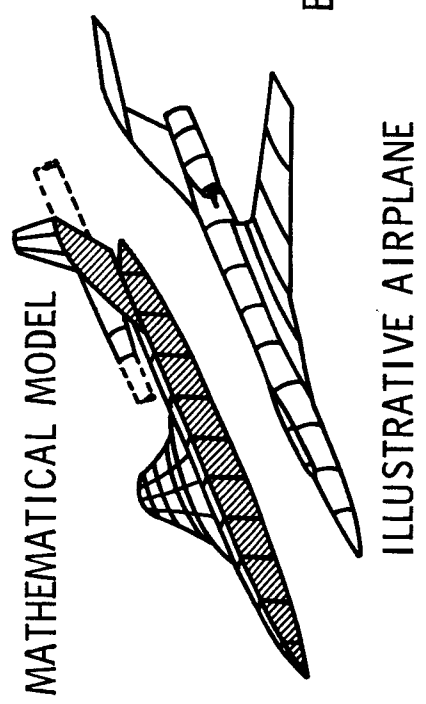
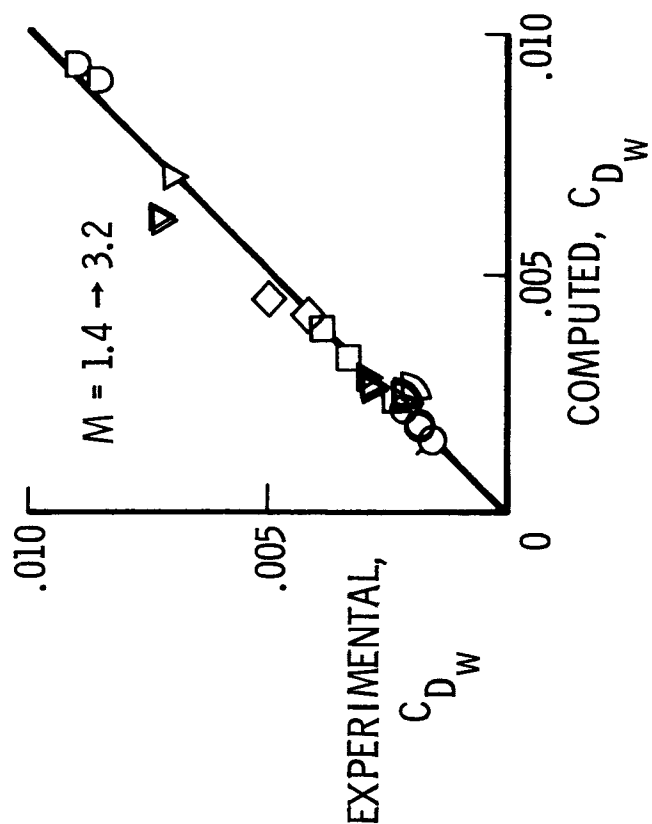


Figure 1.- Zero-lift wave drag.

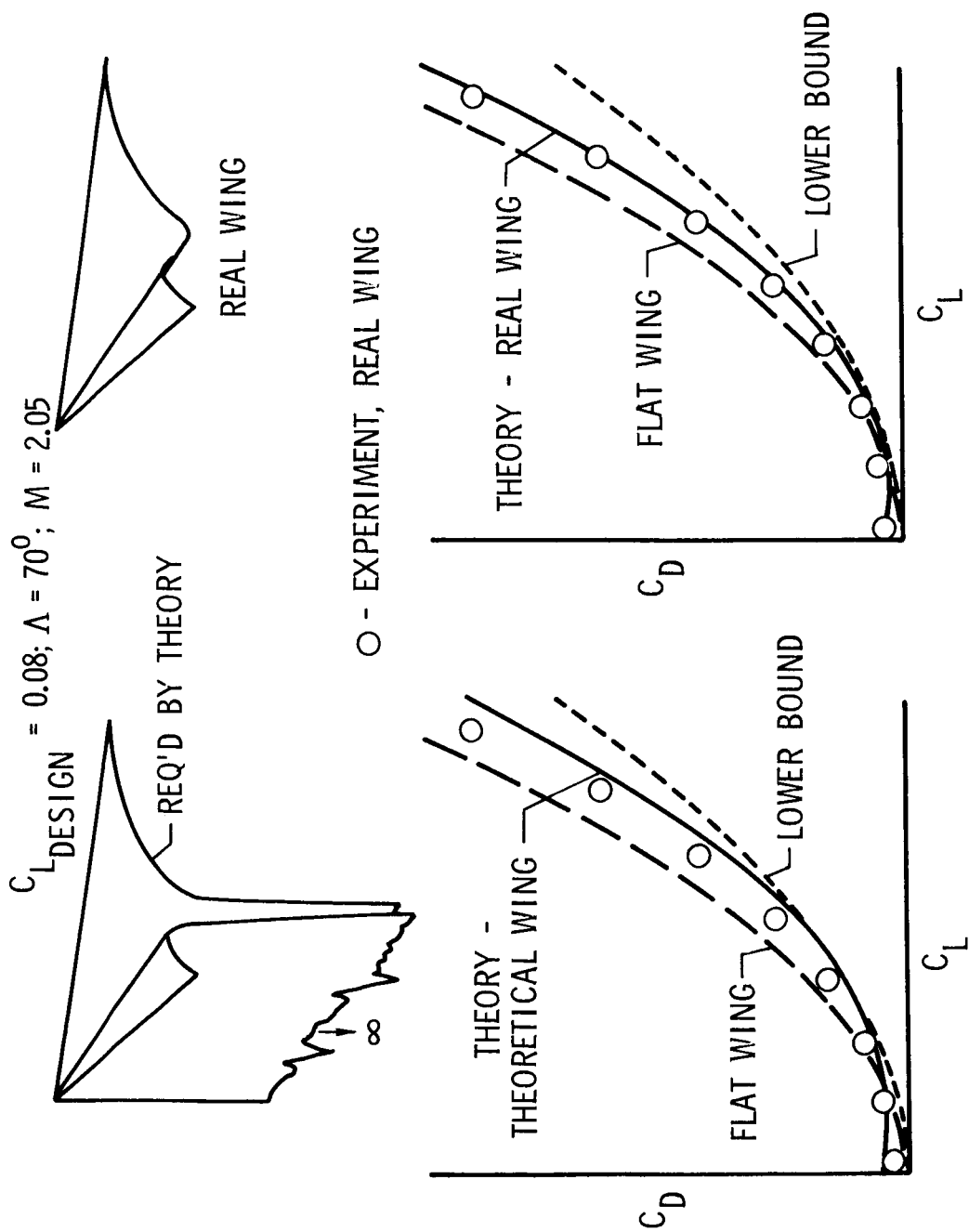


Figure 2.- Drag due to lift: Real and theoretical wings.

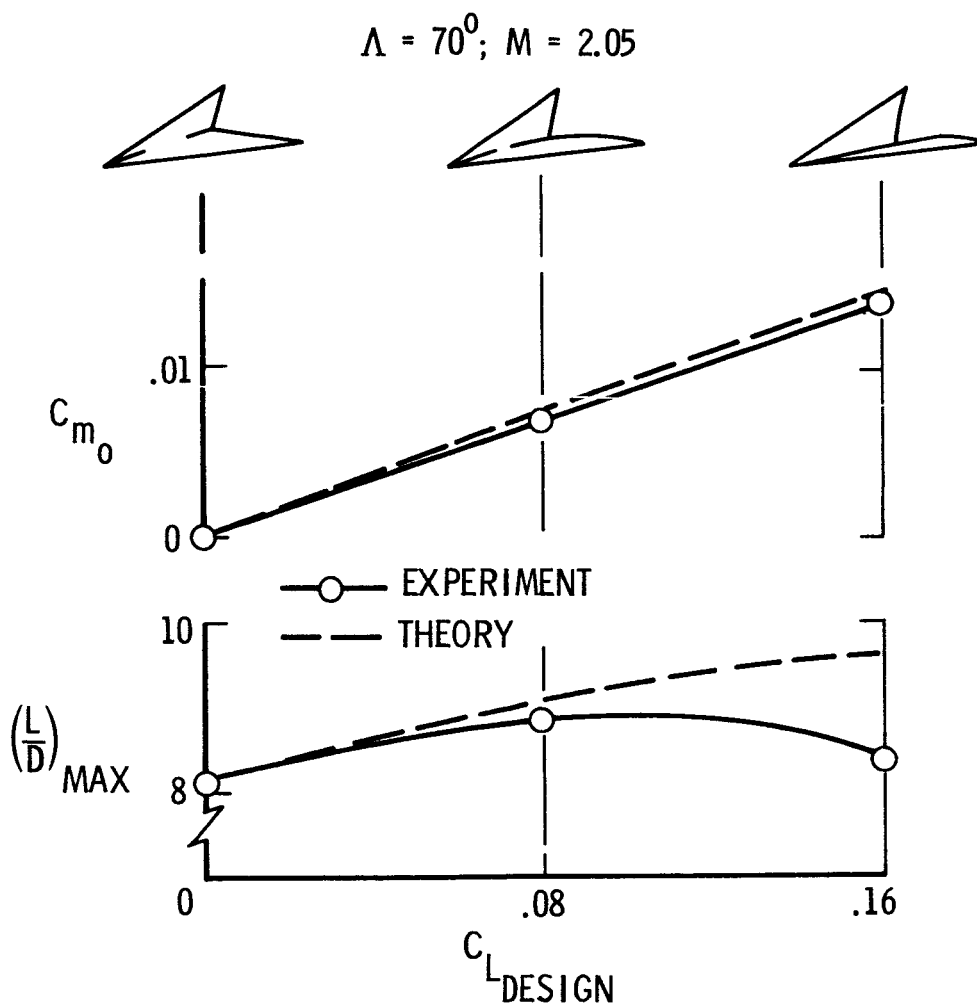


Figure 3.- Effect of wing warp on maximum L/D and zero-lift pitching moment.

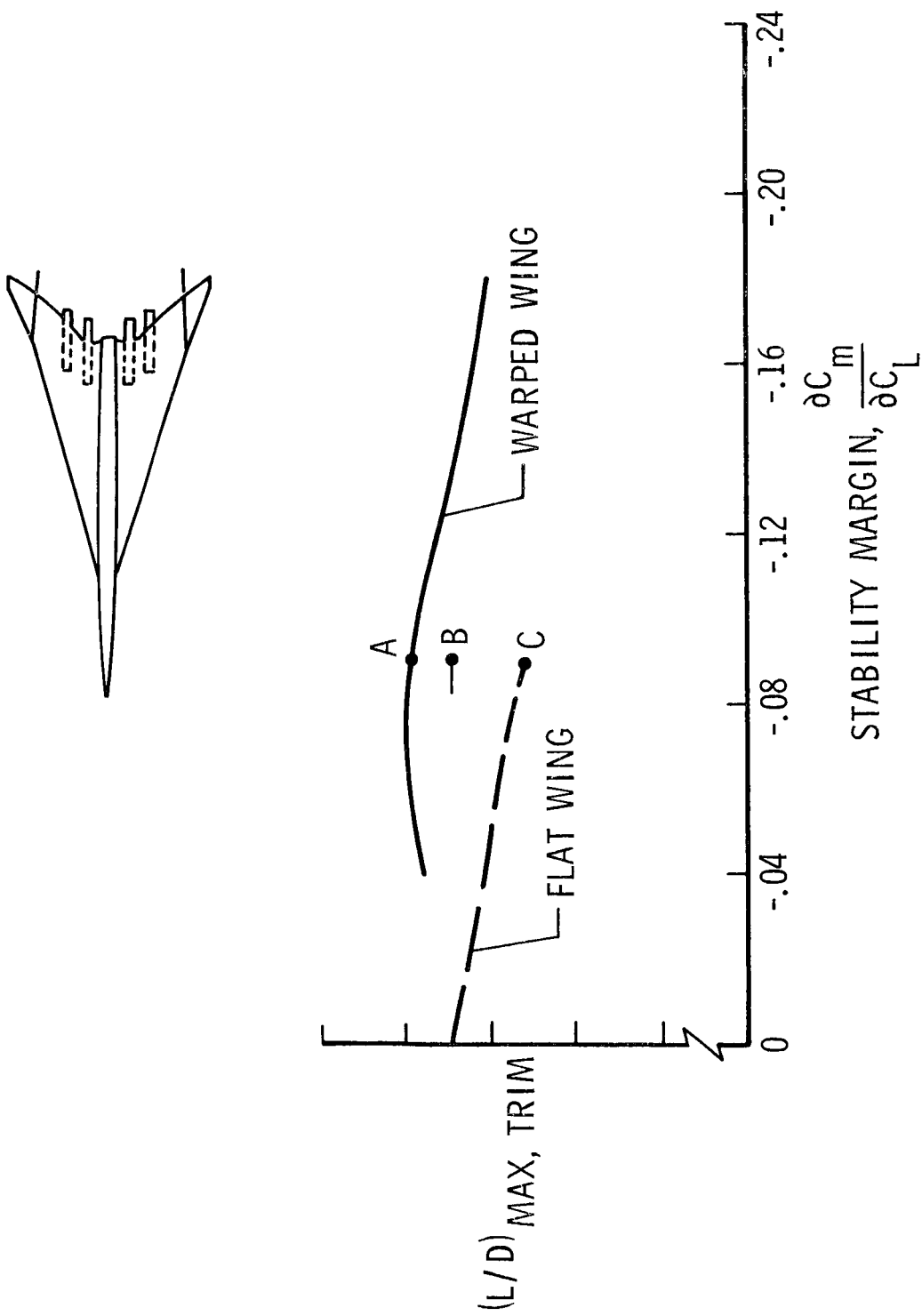


Figure 4.- Effect of wing warp on trim characteristics: $M = 2.6$.

A - SYMMETRIC, NONINTERFERENCE CASE

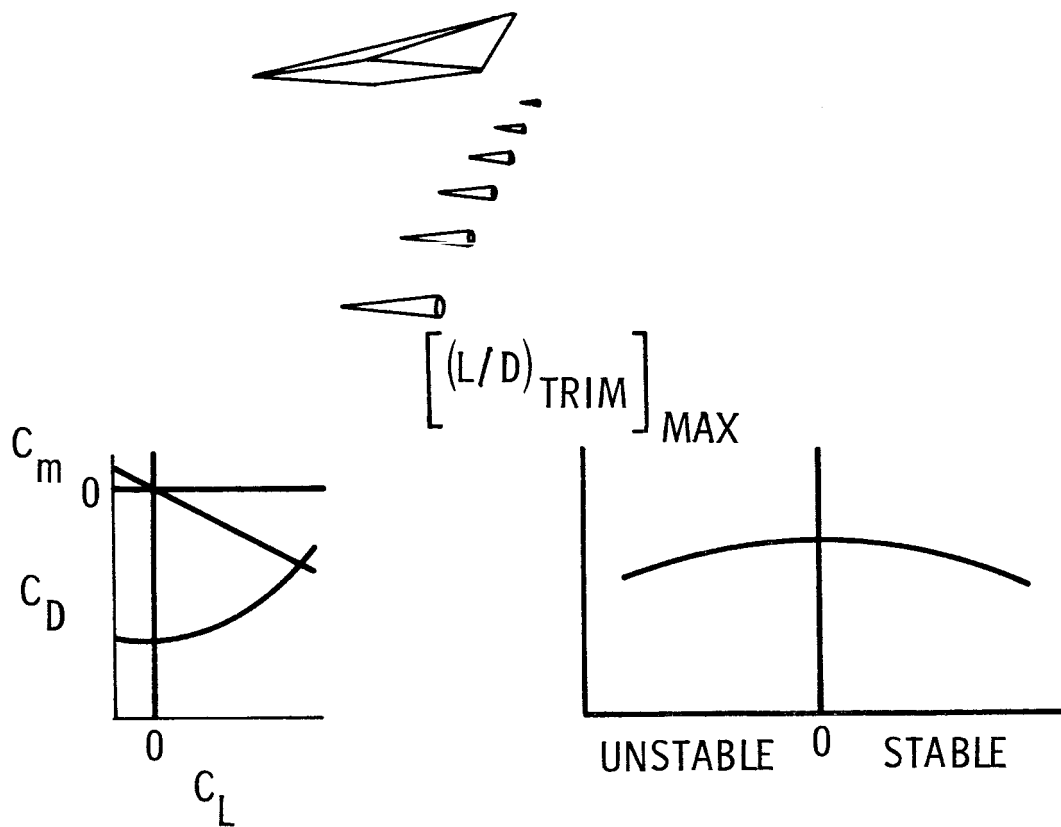
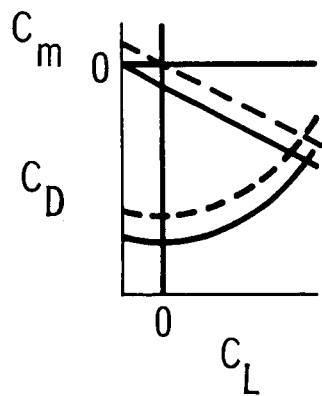
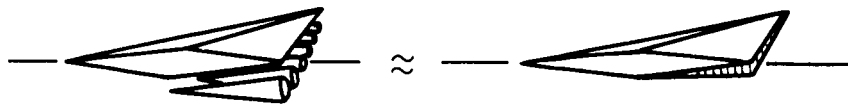


Figure 5.- Interference considerations.

B - FAVORABLE INTERFERENCE, UNREFLEXED-WING CASE



$[(L/D)_{\text{TRIM}}]_{\text{MAX}}$

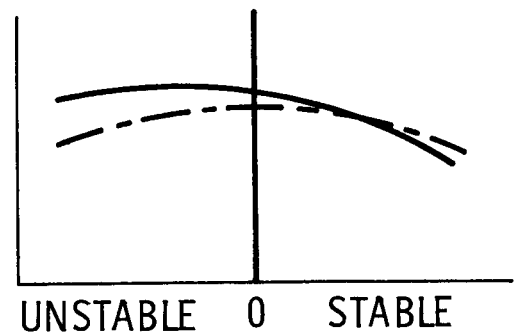


Figure 6.- Interference considerations.

C - FAVORABLE INTERFERENCE, REFLEXED-WING CASE

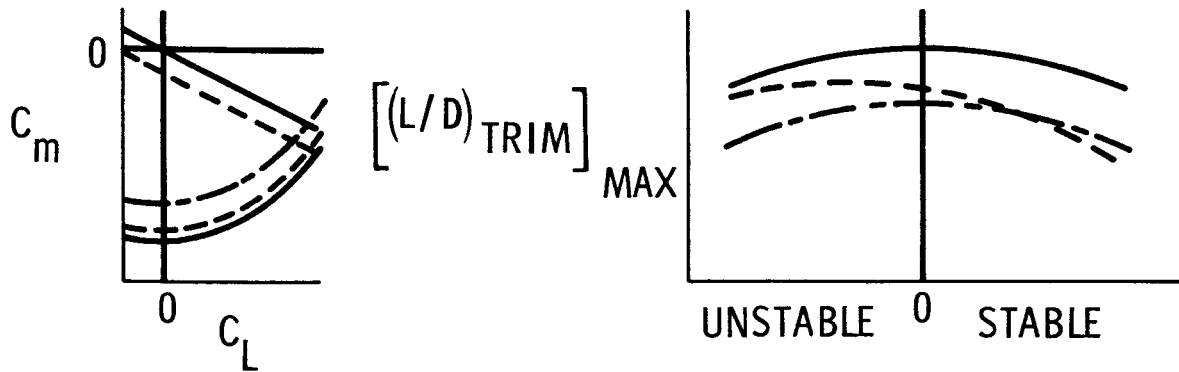
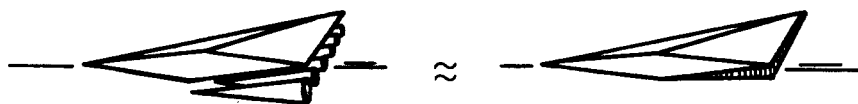


Figure 7.- Interference considerations.

CONDITION

- NO INTERFERENCE
- FAVORABLE INTERFERENCE
- FAVORABLE INTERFERENCE + REFLEX
- FAVORABLE INTERFERENCE + REFLEX

CAMBER SHAPE

- FLAT
- FLAT
- FLAT
- WARPED

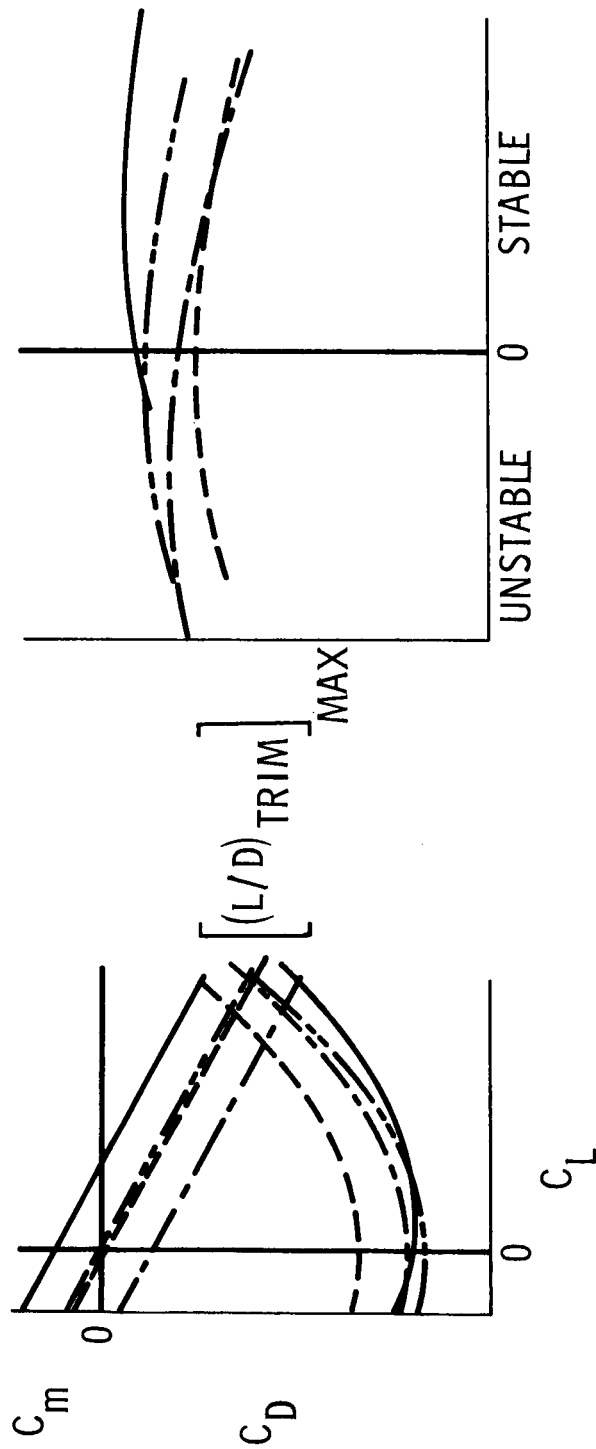


Figure 8.- Interference considerations.

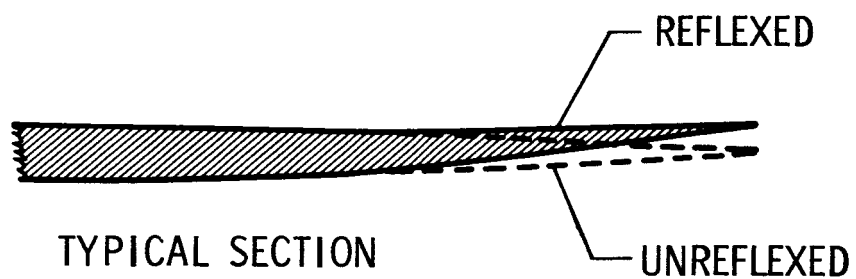
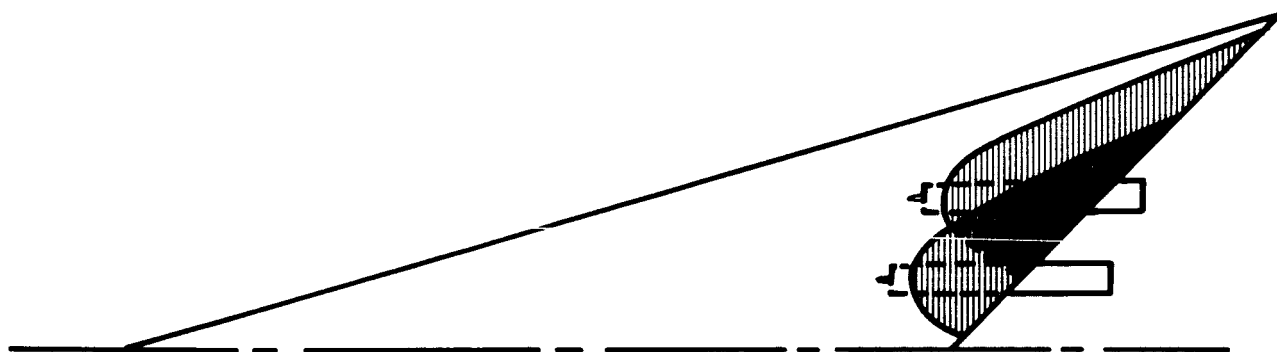


Figure 9.- Wing reflex to accommodate nacelle interference.

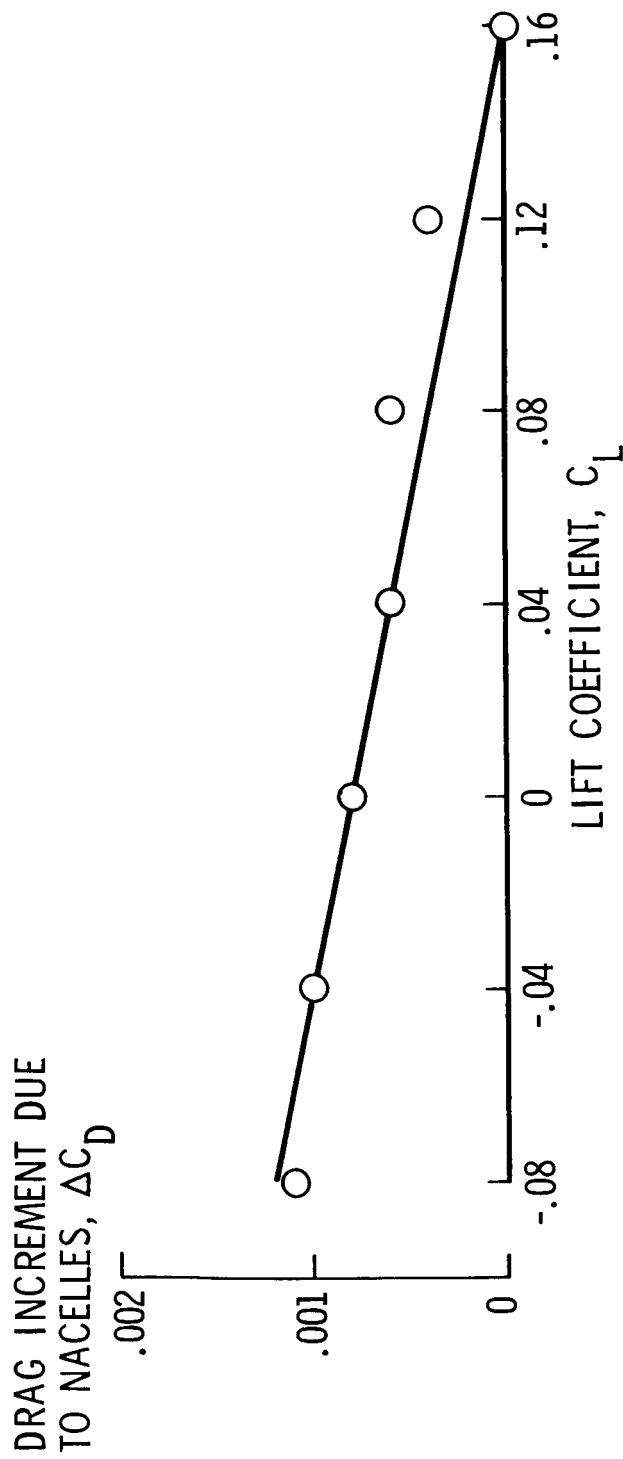


Figure 10.- Effect of lift on nacelle drag increment.

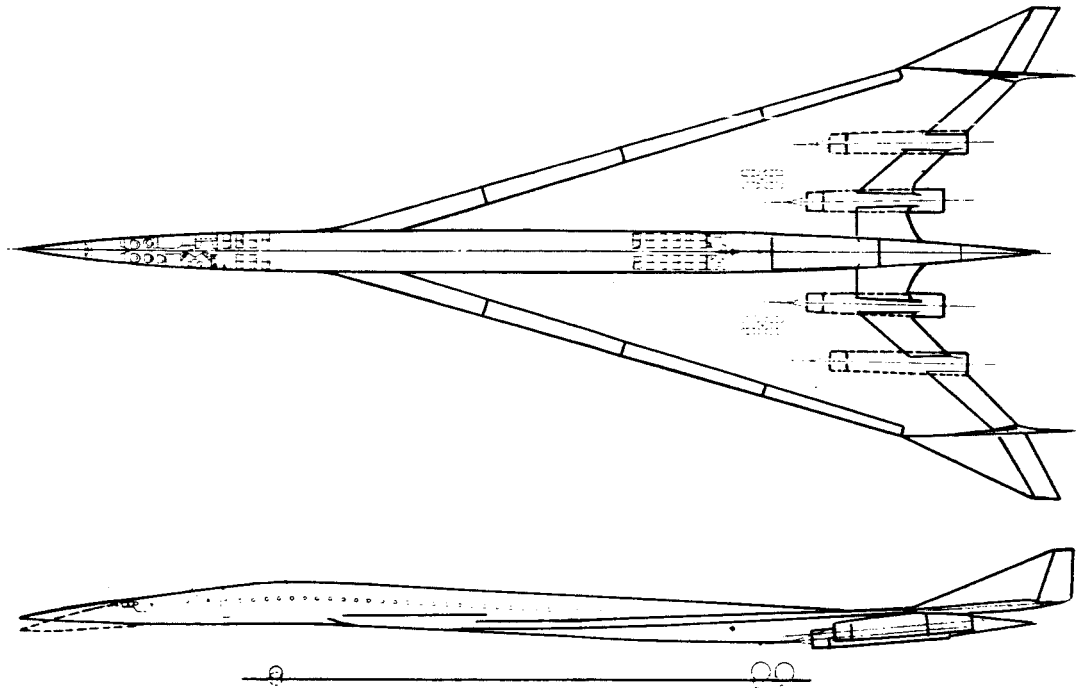


Figure 11.- Scat 15-F configuration.

SCAT 15-F MODEL AT $M = 2.6$

EXPERIMENT	THEORY	CONFIGURATION
○	—	WARPED WING + BODY
□	- - -	FLAT WING + BODY
◇	- - -	REFLEXED WARPED WING + BODY + V TAILS
△	- - -	REFLEXED WARPED WING + BODY + V TAILS + NACELLES

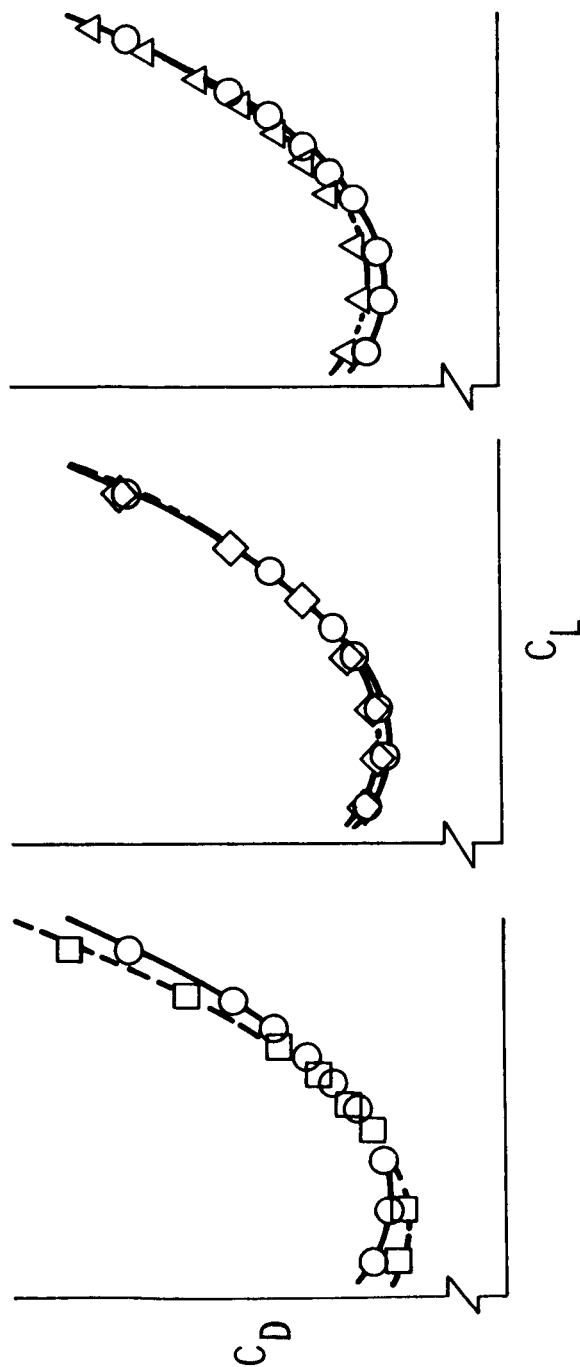


Figure 12.- Experimental and theoretical drag buildup.